Thermodynamics of fractal spectra: Cantor sets and quasiperiodic sequences

P. Carpena,[1,2] A. V. Coronado,[2] and P. Bernaola-Galván[2,3]
[1]*Theoretical Physics, Oxford University, 1 Keble Road, OX1 3NP Oxford, England*
[2]*Departamento de Física Aplicada II, Universidad de Málaga, Málaga, Spain*
[3]*Center for Polymer Studies and Department of Physics, Boston University, Boston, Massachusetts 02215*
(Received 27 May 1999; revised manuscript received 28 September 1999)

We study the properties of the specific heat derived from fractal spectra, for which we extend and generalize some previous known results concerning the log-periodic oscillations of the specific heat $C(T)$. For the monoscale case, we obtain analytically the behavior of $C(T)$ for a two-branch general spectrum, and we show that the oscillatory regime becomes nonharmonic if there exist different gap sizes. In the multiscale case, we connect the role of the spectral dimension as the average value of $C(T)$ with the multifractal properties of the sets, and we give a condition for which the oscillatory regime disappears. Finally, we study the thermodynamics of tight-binding Fibonacci spectra, which are not strictly invariant under changes of scale, and then many of the properties found in Cantor sets become in this case just approximated.

PACS number(s): 05.20.−y, 61.44.Br, 61.43.Hv

I. INTRODUCTION

The experimental discovery of quasicrystals by Shechtman *et al.* [1] produced a great interest in the understanding of the properties of these systems, as is shown by the great amount of theoretical and experimental work that followed. In general, quasicrystals present intermediate properties between pure periodic structures (Bloch systems) and random materials, in spite of the purely deterministic rules used to generate them. To gain a physical insight into the general properties of these materials, the case of one dimensional sequences have been extensively studied, such as Fibonacci, Thue-Morse, prime numbers, and many others. They are known in general as quasiperiodic sequences, and have even been realized experimentally in superlattices [2,3]. The behavior of electrons, photons, phonons, and other particles or quasiparticles has been and is currently being studied in quasiperiodic sequences [4–12], and interest is still increasing.

The general property, and perhaps the most characteristic one, shared by all quasiperiodic sequences is a *fractal energy spectrum*. These spectra, however, tend to be very complex, and simplified fractal models have been used to explain their properties. In a recent paper, Tsallis *et al.* [13] studied the *triadic Cantor set* (a monoscale fractal) in order to clarify the thermodynamic properties of these kind of spectra, and they centered the study in the properties of the specific heat, which presents oscillations around the fractal dimensionality of the spectrum. After that, Vallejos *et al.* [14] extended the study to a two-scale fractal set, showing that in this case, the specific heat also exhibits log-periodic oscillations around the spectral dimension of the system.

In this paper, first we explain how to construct generalized Cantor sets, which can be monoscale or multiscale sets. After that, we center our attention in general monoscale generalized Cantor sets, for which we study numerical and analytically the properties of the specific heat, generalizing the monoscale results of [13]. Then, we analyze the multiscale case by showing first the results obtained in [14]. We connect these results with the properties of the multifractal spectrum of the system, and we include some additional results, indicating in which conditions the oscillatory regime disappears. Once the results for these idealized spectra are known, we study the specific heat obtained from a ''realistic'' fractal spectra: we diagonalize Fibonacci tight-binding models, and by starting from the eigenvalues spectra as we have done before with Cantor sets, we calculate the specific heat and we interpret the results according to the properties previously found in the Cantor sets case.

II. GENERALIZED CANTOR SETS

In the following, we consider a bounded energy spectrum ranging from 0 to Δ, the bandwidth. Without loss of generality, we take the case $\Delta=1$. A generalized Cantor Set can be generated iteratively as follows. In the step $n=0$ of the generation process we have the continuous segment [0,1]. To generate the set (note the nomenclature) $S(j,m)$, in the step $n=1$ we divide the initial segment into j(j integer) identical subsegments of length j^{-1}, labeled from 0 to $j-1$. Then we eliminate $j-m$ segments, thus leaving m subsegments ($m<j$) in the spectrum. In order to maintain the total width Δ of the spectrum, the segments 0 and $j-1$ cannot be eliminated. Note that, given j and m, there are $\binom{j-2}{m-2}$ different ways of choosing the m subsegments [and therefore $\binom{j-2}{m-2}$ different $S(j,m)$]. To distinguish between them we propose the following notation:

$$S(j,m;c_1,c_2,\ldots,c_m), \tag{1}$$

where $\{c_1,c_2,\ldots,c_m\}$ is the set of labels of the segments which are not eliminated. According to the restrictions imposed above, it is clear that they must verify $0=c_1<c_2<\ldots<c_m=j-1$. Once one of these possible ways is chosen, it has to be maintained throughout the generation process, in order to get a fractal structure. It is important to point out here that, when eliminating $j-m$ segments, the remaining spectra is not necessarily formed by m branches. We will have a spectrum of total length $m\times j^{-1}$, but some of the m segments could be contiguous. The segments that are contiguous form a unique spectral branch. In the following step of the generation $n=2$, we take each one of the *branches* (not segments) resulting from the previous step, and we di-

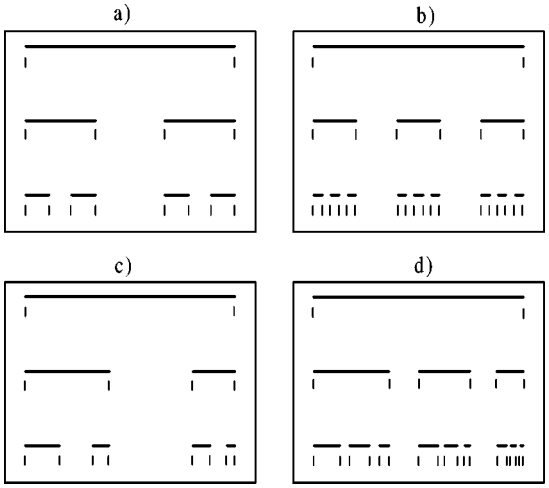

FIG. 1. Four generalized Cantor sets in the first three steps of the generation process. We show the banded (continuous) and discrete case for the sets (a) $S(3,2;0,2)$, (b) $S(5,3;0,2,4)$, (c) $S(5,3;0,1,4)$, and (d) $S(8,5;0,1,2,4,5,7)$.

vide it into j subsegments, and eliminate $j-m$ subsegments *in the same order* as we did in the previous step. The process continues iteratively to generate the fractal. Note that we have just considered the case in which the length of any spectral branch is given by a rational number (the segment $[0,1]$ is divided into an integer number of parts). This is done for the sake of simplicity, but the results obtained are completely general.

In Fig. 1 we show some Cantor sets in the first three steps of generation, and, at the same time, this figure allows us to define graphically discrete and banded spectra, following the nomenclature of [13]. The banded case corresponds to considering the spectrum as formed by continuous branches (the solid line segments in Fig. 1) with constant density of states, separated by gaps with zero density of states. In the discrete case, the spectrum is formed just by the extrema of such branches. The spectra shown in Fig. 1 correspond to the sets (a) $S(3,2;0,2)$, (b) $S(5,3;0,2,4)$, (c) $S(5,3;0,1,4)$, and (d) $S(8,5;0,1,2,4,5,7)$. Note that the standard triadic Cantor set is given by $j=3$, $m=2$, and as $\binom{3-2}{2-2}$, this set is the only $S(3,2)$.

Monoscale and multiscale generalized Cantor sets

In case (b) of Fig. 1, after eliminating $(j-m)$ segments, the m $(m=3)$ remaining segments of length j^{-1} $(j=5)$ in the first step (j^{-n} in the nth step) are *nonadjacents*, i.e., they are separated by gaps. Thus, each segment gives rise to a distinct spectral branch, and as a direct consequence, all the branches have the same length. In this sense, we have a *monoscale* fractal set: in a general step n of the generation process, all the branches forming the spectrum are identical. Clearly, case (a) in Fig. 1 [the triadic Cantor set $S(3,2)$] is also a monoscale fractal.

Nevertheless, case (c) is different. Note that although $m=3$ and $j=5$ as in (b), now in the step $n=1$ we eliminate segments number 2 and 3. Therefore, we have segments 0, 1, and 4 remaining in the spectrum. But in this case, segments 0 and 1 are *adjacent*, and therefore both give rise just to a single spectral branch of size 2×5^{-1}, while segment 4 originates a branch of size 5^{-1}. As the generation process repeats the same division and segment selection *in each branch*, we propagate the two different scales forming a *multiscale* fractal. As an additional example, in case (d) we form one of the sets $S(8,5;0,1,2,4,5,7)$ by eliminating segments number 3 and 6 thus creating three branches of sizes 3×8^{-1}, 2×8^{-1}, and 8^{-1}, respectively. We have now a three-scale fractal. It is clear that more complicated and multiscale sets can be constructed just by taking appropriate values of j, m and by choosing properly the set $\{c_1,c_2,\ldots,c_m\}$.

Finally, we want to include the expression for the fractal dimension (box-counting dimension) d_{box} for generalized Cantor sets. For the general monoscale $S(j,m;c_1,\ldots,c_m)$, it is easy to obtain that $d_{\mathrm{box}}=\log m/\log j$. For multiscale $S(j,m;c_1,\ldots,c_m)$, it is slightly more complicated. It can be shown (see, for example, [15]) that if the spectrum is formed in the first step of generation by n branches, each one of length l_i, the dimension d_{box} is given by the solution of the following equation:

$$\sum_{i=1}^{n} l_i^{d_{\mathrm{box}}}=1. \tag{2}$$

III. ELEMENTS OF THE SETS: ENERGY SPECTRA

In this section, we give an explicit expression for the energy spectrum of the general set $S(j,m;c_1,c_2,\ldots,c_m)$ for the discrete case (see Fig. 1). We restrict ourselves to the discrete case, because in the limit $n\to\infty$ both cases must coincide. The first step is to note that the set formed by the smallest energy of any interval of a generalized Cantor set in the nth step of generation (that we term from now on as E_n^-) can be obtained from the following expansion:

$$E_n^-=\left\{\sum_{k=1}^{n}\frac{c_k}{j^k}\right\}, \tag{3}$$

where each of the coefficients c_k can take all the possible values in $\{c_1,c_2,\ldots,c_m\}$. Similarly, it is easy to see that the set of the highest energies of any interval in a generalized Cantor set (termed E_n^+) is given by

$$E_n^+=\left\{\sum_{k=1}^{n}\frac{c_k}{j^k}+\frac{1}{j^n}\right\}. \tag{4}$$

Note that the set of numbers $\{c_1,c_2,\ldots,c_m\}$ determine completely these energies at all levels of construction of the fractal. In particular, for the triadic Cantor set we have $c_k=0$ or $c_k=2$. Value 0 allows the generation of the first branch of the spectrum, and value 2 the last one. Value 1 would generate the central third of any branch of the spectrum at all scales, which is eliminated. Moreover, it is straightforward to see that for all monoscale Cantor sets we have

$$S_n(j,m;c_1,c_2,\ldots,c_m)=E_n^-\cup E_n^+. \tag{5}$$

In the case of multiscale Cantor sets, a little subtlety has to be taken into account. As two consecutive subsegments are allowed to be taken together in the generation process,

the end of the first one, which is also the beginning of the second, is eliminated from the spectrum, because these two segments form a unique branch. The same argument can be applied if more than two subsegments are taken together. These points $E^{+,-}$ to be eliminated are then the ones which satisfy the relation $E^{+,-}=E_n^- \cap E_n^+$. Therefore, the more general expression for a generalized Cantor set energy spectrum is

$$S_n(j,m;c_1,c_2,\ldots,c_m)=E_n^- \cup E_n^+ - E_n^- \cap E_n^+ . \qquad (6)$$

Note that this equation is valid in all cases, because for monoscale sets $E_n^- \cap E_n^+ = \varnothing$, and then Eq. (6) is reduced to Eq. (5).

IV. MONOSCALE CANTOR SETS THERMODYNAMICS

In this section, we will calculate analytically the partition functions Z for monoscale Cantor sets energy spectra, from which we will obtain the specific heat $C(T)$. For a monoscale Cantor set, analytical expressions can be derived for the thermodynamical functions. Regarding the energy spectra given by Eq. (5), the partition function for the monoscale $S(j,m;c_1,c_2,\ldots,c_m)$ in the nth step of the generation process can be obtained as

$$Z_n(T)=\sum_{c_1,c_2,\ldots,c_n=c_1,c_2,\ldots,c_m}\left\{\exp\left[-\beta\left(\sum_{k=1}^{n}\frac{c_k}{j^k}\right)\right]+\exp\left[-\beta\left(\sum_{k=1}^{n}\frac{c_k}{j^k}+\frac{1}{j^n}\right)\right]\right\}, \qquad (7)$$

where the expressions for the sets E_n^- and E_n^+ given by Eqs. (3) and (4) have been taken into account. In this equation, we have used $\beta \equiv 1/k_B T$. From now on, we take $k_B=1$. Note that the indexes of the summation are the coefficients $c_1,\ldots,c_n$, each of them take the m nonconsecutive values of the set $\{c_1,c_2,\ldots,c_m\}$. For brevity, from now on we define $\Sigma_{c_i=c_1,c_2,\ldots,c_m} \equiv \Sigma_{c_i}$.

After some straightforward calculations, the partition function in Eq. (7) can be factorized in a very compact expression,

$$Z_n(T)=\left[1+\exp\left(-\frac{\beta}{j^n}\right)\right]\prod_{i=1}^{n}\left[\sum_{c_i}\exp\left(-\frac{\beta c_i}{j^i}\right)\right]. \qquad (8)$$

From this expression for the partition function, the thermodynamic magnitudes can be derived. In particular, the internal energy can be obtained as $U_n(T)=\beta^{-2}d(\ln Z_n)/dT$. Finally, after some long but straightforward calculation, the specific heat $C_n(T)$ can be obtained by differentiating $U_n(T)$. Thus,

$$C_n(T)=\left[\frac{2j^n}{\beta}\cosh\left(\frac{\beta}{2j^n}\right)\right]^{-2}+\beta^2\sum_{i=1}^{n}\frac{\sum_{c_i}\exp\left(-\frac{\beta c_i}{j^i}\right)\sum_{c_i}c_i^2\exp\left(-\frac{\beta c_i}{j^i}\right)-\left[\sum_{c_i}c_i\exp\left(-\frac{\beta c_i}{j^i}\right)\right]^2}{\left[j^i\sum_{c_i}\exp\left(-\frac{\beta c_i}{j^i}\right)\right]^2}. \qquad (9)$$

Note that the first term of the right-hand side of Eq. (9) can be considered as a finite size correction of the specific heat. In the $n\to\infty$ limit, only the second term is relevant and then we have

$$C_\infty(T)=\beta^2\sum_{i=1}^{\infty}\frac{\sum_{c_i}\exp\left(-\frac{\beta c_i}{j^i}\right)\sum_{c_i}c_i^2\exp\left(-\frac{\beta c_i}{j^i}\right)-\left[\sum_{c_i}c_i\exp\left(-\frac{\beta c_i}{j^i}\right)\right]^2}{\left[j^i\sum_{c_i}\exp\left(-\frac{\beta c_i}{j^i}\right)\right]^2}. \qquad (10)$$

This equation, which is general though rather complicated, can be evaluated numerically to obtain the dependence of the specific heat on temperature. It is also easy to construct numerically the desired spectra, and to sum and differentiate numerically the partition function. Nevertheless, for some special cases, Eq. (10) can be simplified considerably, as we see in the following.

The simplest case of a monoscale Cantor set is the one in which, after dividing the spectral branch into j subsegments, only the first and the last one are selected, i.e., $S(j,2;0,j-1)$. Note that the triadic Cantor set is one of these simple sets. In this case, it is possible to perform the summation Σ_{c_i},

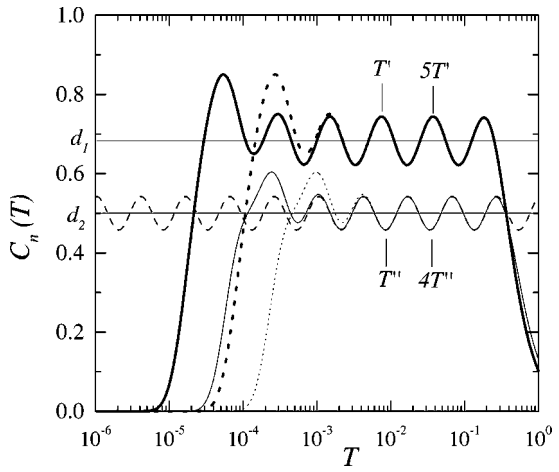

FIG. 2. Finite approximations of the specific heat for the sets $S(5,3;0,2,4)$ (thick lines) and $S(4,2;0,3)$ (thin lines). In both cases, the dotted line corresponds to $n=5$ and the solid one to $n=6$. The horizontal lines represent the correspondent fractal dimensionalities. The dashed line represents $C_\infty^+(T)$ for the set $S(4,2;0,3)$.

and simplify to some extent Eq. (10). Finally, we have

$$C_\infty(T)=\sum_{i=1}^{\infty}\left[\frac{2j^iT}{j-1}\cosh\left(\frac{j-1}{2j^iT}\right)\right]^{-2}. \tag{11}$$

A similar result was obtained for the particular case $j=3$ (the triadic Cantor set) in Ref. [13]. However, note that Eq. (11) is only valid for monoscale sets of the type $S(j,2;0,j-1)$, while for the general monoscale $S(j,m;c_1,c_2,\ldots,c_m)$ Eq. (10) is needed.

In Fig. 2, we show two finite approximations to the specific heat of two monoscale cantor sets as a function of temperature in log-scale. Several important features of the specific heat deserve to be pointed out. First, the specific heat at low T is an *oscillating* function, the number of the oscillations being controlled by the ''depth'' of the fractal, i.e., the step in the generation process. Note that the number of ''periods'' in each case coincides with n, and when n increases, a new period appears in the low T region. Second, $C_n(T)$ oscillates around a particular value given by the fractal dimensionality of the set. In the cases shown in Fig. 2, we have $d_1=\log 3/\log 5$, and $d_2=\log 2/\log 4$. In the general case, we have that the oscillations are around $d=\log m/\log j$. Third, note that in the oscillating regime, $C_n(T)$ is a *log-periodic* function. We have marked some special temperatures in Fig. 2 to indicate this fact. In general, the period of the oscillations for the monoscale set $S(j,m;c_1,c_2,\ldots,c_m)$ is given by j, i.e., $C_n(T)=C_n(jT)$. We discuss on an analytical basis the reasons for this periodicity following Eq. (14). This ''periodicity'' is only valid in the oscillating regime. In the case $n\to\infty$, this regime extends infinitely (infinite number of periods) from approximately $T=1$ towards $T=0$. In the high T limit, the specific heat tends to zero, this is a consecuence of having a bounded spectrum ($E=1$ is the greatest value of the energy).

The limit $T\to\infty$ can be performed in Eq. (10) to obtain the behavior of the specific heat in this region. In this case, we obtain

$$C_\infty(T\to\infty)\simeq\frac{m\sum_{c_i}c_i^2-\left(\sum_{c_i}c_i\right)^2}{m^2(j^2-1)}\,\frac{1}{T^2}. \tag{12}$$

This equation shows how the parameters of the Cantor set, j, m, and the set of values $\{c_1,c_2,\ldots,c_m\}$ control not only the ''average'' value $\log m/\log j$, but also the behavior in the high T limit, entering as the coefficient of T^{-2}.

For the simplest cases $S(j,2;0,j-1)$ is easy to see from Eq. (11) that in the $T\to\infty$ limit we have

$$C_\infty(T)\simeq\frac{(j-1)^2}{4T^2}\sum_{i=1}^{\infty}j^{-2i}=\frac{(j-1)^2}{4(j^2-1)}\,\frac{1}{T^2}. \tag{13}$$

Of course, the same result could be obtained from Eq. (12) taking into account that in the simplest case $m=2$ and any c coefficient just can take the values 0 and $j-1$.

If we generate the fractal also towards higher scales of energy instead of restricting ourselves to the interval $[0,1]$, we can avoid the behavior $C_\infty\to 0$ in the $T\to\infty$ limit. Note that to achieve this, it is enough to consider not only negative integer powers of j (i.e., propagating the fractal to small scales) but also positive ones. In this case, we propagate the fractal structure to the whole positive real axis. All the equations we have seen in this section remain valid just by changing the summation $\Sigma_{i=1}^{n}$ by $\Sigma_{i=-n}^{n}$ for the finite n step of generation, or equivalently in the infinite case, $\Sigma_{i=1}^{\infty}$ by $\Sigma_{i=-\infty}^{\infty}$. From now on, we will term as C_∞^+ the specific heat obtained by considering that the spectrum without an upper limit. We will study C_∞^+ in order to explain the oscillations around the fractal dimension and the log-periodicity. For the sake of simplicity in writing the equations, we will restrict ourselves to calculating $C_\infty^+(T)$ for the simplest case $S(j,2;0,j-1)$, although the results obtained are general for monoscale sets.

The log-periodicity can be seen easily. Note that when considering $C_\infty^+(T)$, Eq. (11) transforms simply to give

$$C_\infty^+(T)=\sum_{i=-\infty}^{\infty}\left[\frac{2j^iT}{j-1}\cosh\left(\frac{j-1}{2j^iT}\right)\right]^{-2}. \tag{14}$$

This equation shows the log-periodicity, because we have directly $C_\infty^+(j^kT)=C_\infty^+(T)$, for k integer. In this case, the periodicity is valid in the whole real positive axis, and not only in the low T region.

In order to show analytically the reason for the oscillations around the fractal dimension, we can try to sum Eq. (14) by using Poisson's summation rule: $\Sigma_{i=-\infty}^{\infty}f(i)=\Sigma_{k=0}^{\infty}\int_{-\infty}^{+\infty}\exp(2ikx)f(x)dx$. After some calculations, with the change of variable $h=(j-1)/2j^iT$ and taking into account for the $k=0$ term that $\int_0^\infty h\cosh^{-2}h\,dh=\ln 2$, we arrive at

$$C_\infty^+(T)=\frac{\ln 2}{\ln j}+\frac{2}{\ln j}\sum_{k=1}^{\infty}\{\alpha_k\cos[2\pi kf(j,T)] -\beta_k\sin[2\pi kf(j,T)]\} \tag{15}$$

with the definitions

$$\alpha_k \equiv \int_0^\infty \frac{h}{\cosh^2 h} \cos\left(\frac{2\pi k \ln h}{\ln j}\right) dh, \tag{16}$$

$$\beta_k \equiv \int_0^\infty \frac{h}{\cosh^2 h} \sin\left(\frac{2\pi k \ln h}{\ln j}\right) dh, \tag{17}$$

$$f(j,T) \equiv \frac{\ln[2T/(j-1)]}{\ln j}. \tag{18}$$

The first two terms of Eq. (15) are very precise to describe the behavior of $C_\infty(T)$. For example, for $j=4$ while $\alpha_1 = 3.002\,328\ldots\times10^{-3}$ and $\beta_1 = 2.908\,951\ldots\times10^{-2}$, we have that $\alpha_2, \beta_2 \sim 10^{-14}$, and so on for higher order coefficients. It is clear than the first harmonic is the unique significative contribution, and then, finally one can write

$$C_\infty^+(T) \simeq \frac{\ln 2}{\ln j} + \frac{2}{\ln j}\{\alpha_1 \cos[2\pi f(j,T)] - \beta_1 \sin[2\pi f(j,T)]\}. \tag{19}$$

This equation contains the main information about monoscale Cantor sets specific heat: the oscillations around the fractal dimensionality $\log m/\log j$ ($\log 2/\log j$ in the case we have calculated), and the log-periodicity of $C_\infty^+(T)$, i.e., $C_\infty^+(T) = C_\infty^+(j^k T)$. To illustrate the properties of $C_\infty^+(T)$, in Fig. 2 we also show for the set $S(4,2;0,3)$ the function $C_\infty^+(T)$ given by Eq. (19) as a dashed line.

The analytic result (19) has been obtained for the general monoscale set $S(j,2;0,j-1)$ formed by two spectral branches. If a monoscale with more than two spectral branches is considered, the specific heat oscillates also around $d_{\rm box}$, with a period given by j. But in this case, the analytical calculation becomes much more complicated, so in the following we study some properties of the problem numerically.

One can construct easily different monoscale Cantor sets with the same fractal dimensionality (and then with the same number and size of spectral branches) just by changing the size of the gaps between these branches. For instance, let us consider the two sets $S(9,3;0,2,8)$ and $S(9,3{:}0,4,8)$. Both sets share the same fractal dimensionality ($d_{\rm box} = \log 3/\log 9 = 1/2$), but their correspondent specific heats behave differently. In Fig. 3 we plot the specific heat for a finite approximation ($n=6$) to the sets $S(9,3;0,2,8)$ (solid line) and $S(9,3{:}0,4,8)$ (dotted line). The main difference between them is the amplitude of the oscillations around $d_{\rm box} = 1/2$ (horizontal line in Fig. 3). This amplitude depends on the value of the sum Σ_{c_i}, which reflects the different structure of the sets.

But the amplitude of the oscillations is not the only difference between the two sets. The set $S(9,3{:}0,4,8)$ is in some sense more symmetric than $S(9,3;0,2,8)$, because in the former both gaps and branches have the same size, which is not true in the latter. These geometric differences appear also in the ''harmonicity'' of the specific heat. When the set is symmetric, the oscillatory regime is very harmonic, and only the first harmonic presents a significative contribution. This fact generalizes the analytic result (19) (obtained for the simplest symmetric case). On the other hand, when the set presents asymmetries, higher harmonics begin to contribute to the oscillations. This is the case of $S(9,3;0,2,8)$, where the two gaps have different size. In Fig. 4 we plot the numerical Fourier transform of the oscillatory regime of the two specific heats of Fig. 3. It can be seen in part (b) that the second harmonic becomes relevant for the oscillations of the specific heat of $S(9,3;0,2,8)$. These results are general: with increasing asymmetries, higher harmonics contribute to the oscillations.

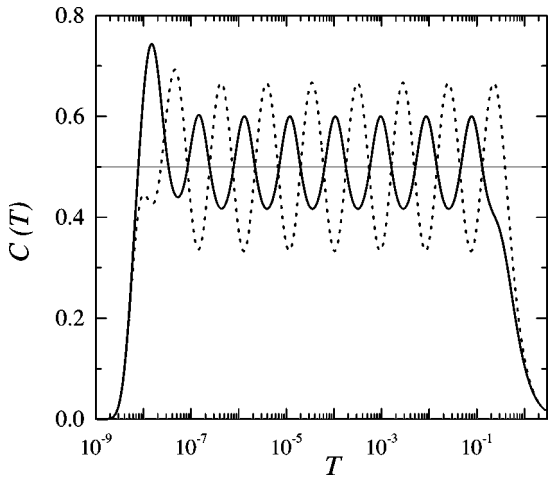

FIG. 3. Plot of the specific heat obtained for a finite approximation ($n=6$) of the sets $S(9,3;0,2,8)$ (solid line) and $S(9,3;0,4,8)$ (dotted line). The horizontal line corresponds to $d_{\rm box}=1/2$.

In the construction of a monoscale Cantor set, we have not considered the possibility of taking together two consecutive segments of length j^{-n} in the nth step of the generation process in order to avoid multiscales. Thus, the sets are formed by m^n branches of size j^{-n}. But even if consecutive segments are allowed to form a spectral branch, a monoscale set can arise if the same is done to generate all the branches. In this case the size of any spectral branch is *not* given by j^{-n}, and then this is not the smallest scale of the allowed spectrum, but it can be the size of the smallest gaps. if in the generation process we start by grouping l segments of length j^{-1} to generate m/l identical branches of length lj^{-1} (note that m/l must be integer to have a monoscale

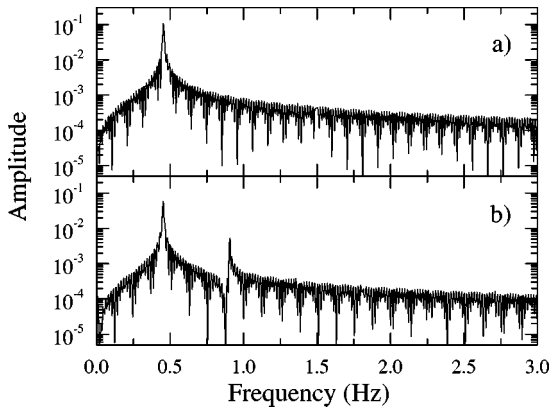

FIG. 4. Plot of the Fourier transform obtained numerically from the oscillatory regime of the specific heats of the sets (a) $S(9,3;0,4,8)$ and (b) $S(9,3;0,4,8)$.

Cantor set), in the nth step of the generation we will have identical branches of size l^n/j^n. The roles of j and m are now played by j/l and m/l. As a consequence, the oscillations of the corresponding specific heat have a periodicity given by j/l. It is also straightforward to see that the fractal dimensionality is given by $d_{\mathrm{box}}=\log(m/l)/\log(j/l)$, and this is also the value around which the specific heat oscillates.

V. MULTISCALE CANTOR SETS THERMODYNAMICS

It is clear that multiscale fractal spectra can be easily constructed by generating appropriate sets $S(j,m)$ [see cases (c) and (d) in Fig. 1]. Unfortunately, although a formal expression can be written for the energy spectrum [Eq. (6)], it is not possible to sum analytically the partition function, and the study of the specific heat has to be done numerically.

In a recent paper, Vallejos *et al.* [14] studied the properties of $C(T)$ for a two-scale fractal spectra, i.e., they considered a spectrum with two branches of sizes l_1 and l_2 corresponding to the low and high energy region, respectively. They gave a scaling argument for the form of the partition function, which led them to obtain the following conclusions: the specific heat presents oscillations around the central value $D=-\log 2/\log l_1$, and the period of these oscillations is given by $1/l_1$. They found a nice interpretation for D. It can be shown that if the integrated density of states $N(E)$ is of the form

$$N(E)\propto E^D, \tag{20}$$

then the average value of the specific heat is given by $\langle C\rangle = D$. This is a generalization of the equipartition principle. For the fractal spectra they studied, the value $D=-\log 2/\log l_1$ is the exponent of a power-law fit of the integrated density of states $N(E)$, also called *spectral dimension*. Then, it is natural for D to be the ''average'' value of $C(T)$ in the temperature range corresponding to the energy range for which Eq. (20) is valid.

Here, we are going to generalize this result for multiscale fractal spectra as follows. When generating a generalized Cantor set, all the branches give rise to the same number of points of the set in the division process. As a consequence, all of these branches have the same weight, given by s^{-1} (where s is the number of branches appearing in the spectrum). Then if l_1 is the length of the leftmost branch of the spectrum, it has a measure (in the multifractal sense) given by $d_{\mathrm{left}}=\log s^{-1}/\log l_1$. When the function $N(E)$ is plotted in a double log-scale, the low energy behavior represented by d_{left} domains always in the power-law fit, so $D=d_{\mathrm{left}}=-\log s/\log l_1$. Note that, in particular, for the sets studied in [14], $s=2$.

As an example, in Fig. 5 we show the function $N(E)$ for the three-scale set $S(8,5;0,2,3,5,6,7)$ ($s=3$). The dotted line represents a power-law fit, with exponent given by $D=\log 3/\log 8=0.528\ldots$. In the inset, we represent the specific heat for a finite approximation ($n=8$) of the same set, showing the oscillations around the spectral dimension D (see below). This example illustrates how in general the spectral dimension is given by $D=-\log s/\log l_1$, where s is the number of branches appearing in the spectrum.

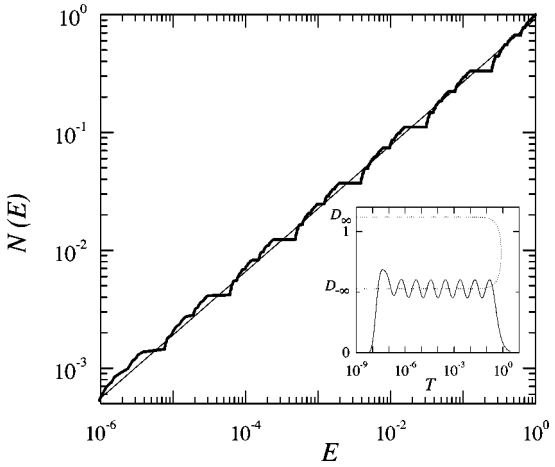

FIG. 5. The function $N(E)$ for the three scale set $S(8,5;0,2,3,5,6,7)$ (solid line). The dotted line represents a power-law fit, with exponent given by $D=\log 3/\log 8=0.528\ldots$. In the inset, we represent the specific heat for a finite approximation ($n=8$) of the same set (solid line). The dotted line represents the multifractal spectrum of the same set.

One can also arrive at that value of D by considering the information of the multifractal spectrum of the corresponding set [15]. If the first spectral branch is the biggest or the smallest one, then the measure will be most rarified or most concentrated exactly in this region. Therefore, the spectral dimension D will coincide with one of the limiting dimensions of the multifractal spectrum, D_∞ or $D_{-\infty}$, respectively. This can be seen also in the inset of Fig. 5, where the dotted line represents the multifractal spectrum obtained for $S(8,5;0,2,3,5,6,7)$. Actually, the oscillatory regime around D is a direct generalization of the monoscale case. In this latter case, all the spectral branches are identical, and then, in particular, we will have $d_{\mathrm{left}}=D=\log s^{-1}/\log l_1=\log m/\log j=d_{\mathrm{box}}$, so the role of D is performed by d_{box}, as we saw in the preceding section.

As can be seen in Fig. 5, $N(E)$ can be considered as a log-periodic oscillating function superimposed to the power-law behavior. The oscillations are strictly log-periodic because the fractal sets we are considering are exactly invariant under changes of scale. Although the oscillations present sharp borders due to the gap structure of the spectrum, Vallejos *et al.* [14] modeled successfully this oscillatory function by a log-harmonic one in the two-scale fractal set, which led directly to the oscillations in $C(T)$. Nevertheless, when a more general multiscale case is considered, we have checked numerically that this approach is not so exact. The reason is the same we found in the general monoscale case: when more than two spectral branches are considered then several gaps exist. If the size of the gaps is different, higher harmonics begin to contribute to the oscillatory regime in $C(T)$, (as was shown in Fig. 4), and therefore these harmonics should be included in the log-periodic oscillatory function that models the spectrum.

Finally, we have encountered numerically a general result concerning the existence or not of the oscillatory regime. We have found a strong dependence of the amplitude of the oscillations on D. As D increases, the oscillations become smaller, and they eventually disappear exactly when $D=1$. For the case $D>1$, no oscillations exist anymore. If a

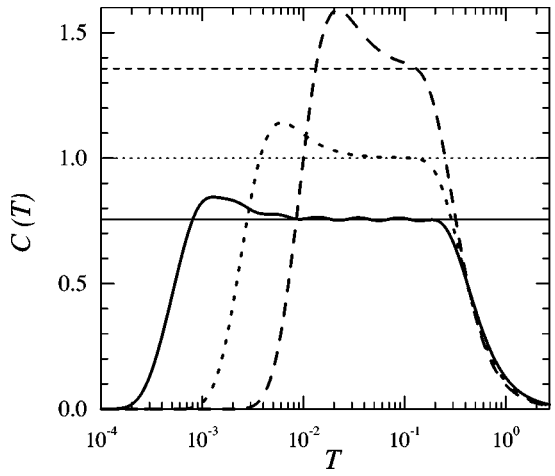

FIG. 6. $C(T)$ for three different sets: $S(5,3;0,1,4)$, for which $D=0.756\ldots$ (solid line), $S(4,3;0,1,3)$, for which $D=1$ (dotted line), and $S(5,4;0,1,2,4)$, for which $D=1.356\ldots$ (dashed line).

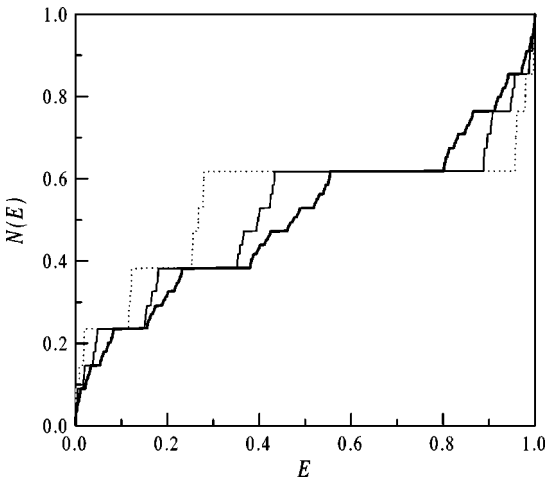

FIG. 7. Integrated densities of states $N(E)$ for a Fibonacci sequence with 987 atoms, and $|\varepsilon_A-\varepsilon_B|=1.5$ (thick line), 3 (thin line), and 6 (dotted line).

s-branches multiscale Cantor set is considered, with l_1 the length of the first one, it is straightforward to see that $D \geqslant 1$ when $l_1 \geqslant 1/s$. Then, the exact critical point where the oscillations disappear is given by the condition

$$l_1 = 1/s. \tag{21}$$

In Fig. 6 we show three examples of $C(T)$ for Cantor sets with D smaller (solid line), equal (dotted line), and greater than unity (dashed line). Note that even when the oscillations disappear, D gives an average value of $C(T)$ in the appropriate range of temperature.

The meaning of Eq. (21) becomes more transparent in monoscale Cantor sets. In this case, it is trivial to see that if $l_1=1/s$, and as all the s branches are equal, then the spectrum becomes continuous (not fractal), formed by the whole segment $[0,1]$.

VI. THERMODYNAMICS OF FIBONACCI SPECTRA

Until now, we have been studying the thermodynamics of ''exact'' and idealized fractal spectra, derived from the construction of Cantor sets. In this section we study the thermodynamics of ''real'' spectra obtained from quasiperiodic sequences. These spectra are just approximately fractal, so we will see how the specific heat is affected by this fact and which is the relation with the ''exact'' spectra. We are going to consider the Fibonacci sequence as the typical quasiperiodic sequence, which is formed by arranging properly two basic building blocks (generically called A and B). The Fibonacci sequence S_∞ is obtained by the recursion relation $S_l=\{S_l S_{l-1}\}$ for $l \geqslant 1$ with $S_0=\{B\}$, and $S_1=\{A\}$. The Fibonacci number F_l is the total number of building blocks A and B in S_l, and obeys the recursion relation $F_{l+1}=F_{l-1}+F_l$ for $l \geqslant 1$ with $F_0=F_1=1$. It is straightforward to see that $S_2=AB$, $S_3=ABA$, $S_4=ABAAB$, and so on. In our case, we are going to consider a nearest-neighbor tight-binding model with the following Hamiltonian for the Fibonacci sequence S_n:

$$H=\sum_{i}^{F_n} \varepsilon_{A(B)}|i\rangle\langle i| + \sum_{\langle i,j\rangle} t|i\rangle\langle j|. \tag{22}$$

In this Hamiltonian, the diagonal energies form a Fibonacci sequence with two basic energies, ε_A and ε_B. The symbol $\langle i,j\rangle$ means that i and j are nearest neighbors, and the hopping term t is considered to be constant. Numerically, we set $t=1$, thus fixing our energy scale. The spectrum of the Hamiltonian (22) is obtained by exact diagonalization of the correspondent matrix.

An appropriate way to see the fractal structure of the spectrum is by using the integrated density of states $N(E)$ [9]. In Fig. 7, we plot three different curves $N(E)$ for three values of the difference $|\varepsilon_A-\varepsilon_B|$ for a Fibonacci system with 987 atoms. All the spectra are normalized to the interval $[0,1]$. As can be seen, the curves resemble very much the shape of the devil staircase, also very similar to the functions $N(E)$ obtained from Cantor sets. The parameter $|\varepsilon_A-\varepsilon_B|$ controls the shape of the spectrum. If $|\varepsilon_A-\varepsilon_B|<t$, the hopping term domains, and the spectrum is still very ''continuous.'' On the contrary, if $|\varepsilon_A-\varepsilon_B|>t$, the quasiperiodicity is stronger, and the spectra are more fractured: the gaps are bigger, and the regions with states smaller. These facts are accentuated as $|\varepsilon_A-\varepsilon_B|$ increases. We will restrict ourselves to the case $|\varepsilon_A-\varepsilon_B|>t$, to appreciate the effects of quasiperiodicity.

Once the set of eigenvalues $\{e_i\}$ is known, we compute the partition function through the usual expression $Z(T)=\Sigma_{i=1}^{F_n}\exp(-e_i/kT)$. From $Z(T)$, we obtain $C(T)$ in the standard way. The specific heat for three different values of $|\varepsilon_A-\varepsilon_B|$ is shown in Fig. 8, corresponding to the spectra shown in Fig. 7. The main feature that can be observed is that the Fibonacci specific heat also presents oscillations (in log-scale) around a certain value, although not in the same exact and regular way as it was found for Cantor sets. The number of oscillations depends on the number of points in the spectra (on the number of atoms in the chain): the bigger the system, the greater the number of oscillations. This is equivalent to the behavior found in generalized Cantor sets,

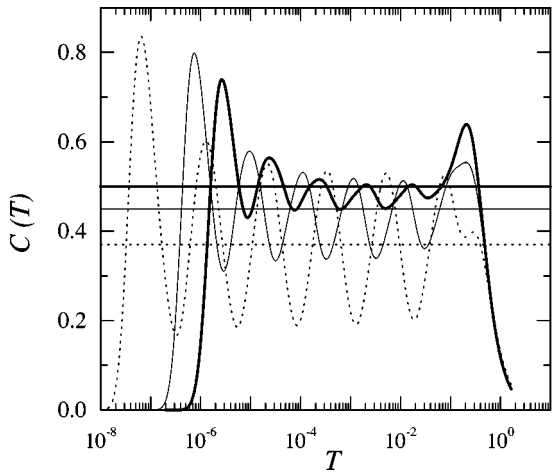

FIG. 8. The specific heat for the spectra shown in Fig. 7, represented with the same type of lines.

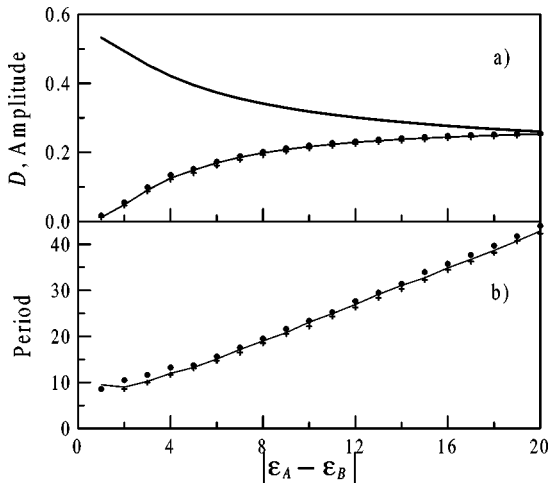

FIG. 9. In (a), the solid thick line represents the value of D, and with a solid thin line, circles, and crosses we represent the amplitudes of three central consecutive oscillations of $C(T)$ both as a function of $|\varepsilon_A-\varepsilon_B|$. In (b), we plot the behavior of the three ''periods'' of the same three oscillations used in (a) with the same type of symbols.

where the oscillations increase with the step of the generation process (the hierarchy of the spectrum).

The horizontal lines in Fig. 8 correspond to the spectral dimensions of the three spectra. The spectral dimensions D depend on the parameter $|\varepsilon_A-\varepsilon_B|$: as it increases and the spectra become more fractured, the spectral dimensions decrease. Note that these dimensions give a good average value of $C(T)$. The reason is that the function $N(E)$ is fitted fairly well in general by a power-law, and then D remains significative. Nevertheless, the ''oscillations'' of $N(E)$ around the power law are not as exact and repetitive as the one found in Cantor sets (represented in Fig. 5). The reason is that the spectra are just approximately fractal: they are not strictly invariant under changes of scale (as it happened for Cantor sets). This fact is reflected in $C(T)$, where different ''periods'' and different ''amplitudes'' can be seen. A general fact is that the first and last oscillations are more irregular, but the central ones are very similar in amplitude and almost periodic. In addition, Fig. 8 shows a clear dependence of the ''period'' and ''amplitude'' of the oscillations on D: both increase as D decreases. As D is controlled by $|\varepsilon_A-\varepsilon_B|$, this is the key parameter of the problem.

In Fig. 9, we show the behavior of all the interesting magnitudes of the problem (D, and period and amplitude of the oscillations) as a function of $|\varepsilon_A-\varepsilon_B|$. In part (a), the solid thick line represents the value of D, and with circles, a solid thin line, and crosses, we represent the amplitudes of three central consecutive oscillations of $C(T)$. Note that, although the amplitudes are not identical, they are very similar and the three curves almost overlap. As expected, D decreases, while the amplitudes increase. It is interesting to see that in the region of very high values of $|\varepsilon_A-\varepsilon_B|$, the limit value of the amplitudes coincide with D. This is logical: as D is the average value, the amplitudes are bounded by D in order to prevent negative values of $C(T)$. In part (b), we present the behavior of three periods (corresponding to the same central oscillations as the previous amplitudes, and with the same symbols) as a function of $|\varepsilon_A-\varepsilon_B|$. Of course, they are periods in ''log'' sense: they are obtained as the quotient between temperatures for which consecutive maxima are reached. As before, the periods are not identical, but very similar, and therefore the curves almost overlap: as the periods are almost the same, in some sense we could say that $C(T)$ is quasi-log-periodic in this region. In addition, there exist a fairly linear dependence of the periods and $|\varepsilon_A-\varepsilon_B|$. Therefore, for very high values of $|\varepsilon_A-\varepsilon_B|$, the oscillations extend over many orders of magnitude, even in the case of small systems.

VII. CONCLUSIONS

In this paper, we have studied the properties of the specific heat derived from fractal spectra. First, we have considered both monoscale and multiscale Cantor sets, for which we have extended and generalized some previous known results concerning the log-periodic oscillations of the specific heat $C(T)$. For the monoscale case, we have obtained analytically the behavior of $C(T)$ for a two-branch general spectrum. By using numerical calculation, we have shown that even in the monoscale case the oscillatory regime becomes nonharmonic if there exist different gap sizes. In the multiscale case, we have studied numerically the case of s branches in the spectrum, where nonharmonicity effects are even more relevant. We have connected the role of the spectral dimension D as the average value of $C(T)$ with the multifractal properties of the sets, and we have found a condition for which the oscillatory regime disappears. After that, we have studied the thermodynamics of tight-binding Fibonacci spectra. These spectra are just approximate fractals (not strictly invariant under changes of scale), and then many of the properties found before in Cantor sets become here just approximated. This fact is specially relevant in the meaning of D, and in the periodicity and amplitude of the oscillations that we have found in the Fibonacci specific heat.

Finally, we would like to connect our results here with some previous works. Examining the vibrational problem, Petri *et al.* [16] and Petri and Ruocco [17], when considering a chain with hierarchical couplings, found integrated densities of states of Cantor sets type. Therefore, some of the

properties found for generalized Cantor sets, derived just from the fractal and scaling properties of the spectra, are expected to be found in their results. For example, although Petri and Ruocco [17] studied the Debye vibrational specific heat, they found small oscillations in the low T region, connected with the results obtained in this paper.

In addition, when studying quasiperiodic spin chains, Luck and Nieuwenhuizen [18] found that the specific heat of a Fibonacci chain oscillates log-periodically with the temperature, which is clearly connected with our results here. Also, Badalian *et al.* [19], when considering a Heisenberg model with quasiperiodic exchange couplings, obtained in some circumstances extra peaks in the specific heat as a function of the temperature in the low T region, also related with the results presented in this paper.

ACKNOWLEDGMENTS

We would like to thank Dr. J. Chalker (Oxford) for a critical reading of the manuscript. P.C. and P.B.G. also thank the Spanish Ministerio de Educación y Cultura for economic support by Grant Nos. PFE-029069359G and PR98-0025095592, respectively.

[1] D. Shechtman, I. Blech, D. Gratias, and J. W. Cahn, Phys. Rev. Lett. **53**, 1951 (1984).
[2] R. Merlin, K. Bajema, R. Clarke, F. Y. Juang, and P. K. Bhattacharya, Phys. Rev. Lett. **55**, 1768 (1985).
[3] T. Hattori, T. Noriaki, S. Kawato, and H. Nakatsuka, Phys. Rev. B **50**, 4220 (1994).
[4] M. Kohmoto, L. P. Kadanoff, and C. Tang, Phys. Rev. Lett. **50**, 1870 (1983).
[5] M. Kohmoto and J. R. Banavar, Phys. Rev. B **34**, 563 (1986).
[6] M. Kohmoto, B. Sutherland, and C. Tang, Phys. Rev. B **35**, 1020 (1987).
[7] C. S. Ryu, G. Y. Oh, and M. H. Lee, Phys. Rev. B **48**, 132 (1993).
[8] E. Maciá, F. Domínguez-Adame, and A. Sánchez, Phys. Rev. B **49**, 9503 (1994).
[9] P. Carpena, V. Gasparian, and M. Ortuño, Phys. Rev. B **51**, 12 813 (1995).
[10] F. Piéchon, M. Benakli, and A. Jagannatan, Phys. Rev. Lett. **74**, 5248 (1995).
[11] P. Carpena, V. Gasparian, and M. Ortuño, Z. Phys. B: Condens. Matter **102**, 425 (1997).
[12] G. G. Naumis, Phys. Rev. B **59**, 11 315 (1999).
[13] C. Tsallis, L. R. da Silva, R. S. Mendes, R. O. Vallejos, and A. M. Mariz, Phys. Rev. E **56**, R4922 (1997).
[14] R. O. Vallejos, R. S. Mendes, L. R. da Silva, and C. Tsallis, Phys. Rev. E **58**, 1346 (1998).
[15] T. C. Halsey, M. H. Jensen, L. P. Kadanoff, I. Procaccia, and B. I. Shraiman, Phys. Rev. A **33**, 1141 (1986).
[16] A. Petri, A. Alippi, A. Bettucci, F. Cracium, F. Farrely, and E. Molinary, Phys. Rev. B **49**, 15 067 (1994).
[17] A. Petri and G. Ruocco, Phys. Rev. B **51**, 11 399 (1995).
[18] J. M. Luck and Th. M. Nieuwenhuizen, Europhys. Lett. **2**, 256 (1987).
[19] D. Badalian, V. Gasparian, R. Abramian, A. Khachatrian, and U. Gummich, Physica B **226**, 385 (1996).